JOURNAL OF CATALYSIS 35, 80–91 (1974)

Role of Structure and Electronic Interactions in the Catalytic Behavior of NiO–TiO$_2$ System

A. M. RUBINSTEIN, A. A. DULOV, A. A. SLINKIN, L. A. ABRAMOVA, I. SH. GERSHENZON, L. A. GORSKAYA, V. JA. DANYUSHEVSKII, M. I. DASHEVSKII, A. L. KLYACHKO-GURVICH, T. K. LAVROVSKAYA, L. I. LAFER, AND V. I. YAKERSON

N. D. Zelinskii Institute of Organic Chemistry, the USSR Academy of Sciences, Moscow, USSR

Received April 30, 1973; revised May 15, 1974

Properties of the coprecipitated NiO–TIO$_2$ catalysts with different NiO/TiO$_2$ ratios (0–100% NiO) have been investigated. X-Ray analysis, electron microscopy, differential thermogravimetry, ir spectroscopy, measurements of adsorption, conductivity, work function, ESR and magnetic susceptibility were the principal methods of study.

Adsorption measurements indicated a maximum on the surface area–composition curve. The enhancement of the surface area is interpreted by applying the concept of mutual protective action. Evidences are presented suggesting that the mutual protection which retards the growth of particles begins to be operative during the coprecipitation step. The possible significance of this phenomenon for the surface properties, structure, and electronic behavior of the catalysts is discussed.

The catalytic properties have been tested for the N$_2$O decomposition. Low catalytic activity of the samples containing as much as 35 mole% of NiO is ascribed to the formation of the low activity nickel titanate layer on the catalyst particles. Isolated Ni^{2+} ions are shown to be inactive for the N$_2$O decomposition. The suggestion is made that local interactions have little, if any, effect on the catalysis under the conditions used.

INTRODUCTION

Present progress in catalysis shows that combined studies are required to establish factors which determine a catalytic process, since the single correlations of the catalytic activity with isolated parameters might be misleading. In the present research we tried to study the NiO–TiO$_2$ system using various methods to gain further insight into the catalytic and physicochemical properties of the nickel catalysts, extensively studied in our laboratory (*1*).

The main object of this study was to find out intimate relationships between properties and chemical composition of the NiO–TiO$_2$ catalysts and to provide a reasonable explanation for the catalytic behavior of these solids.

I. EXPERIMENTAL SECTION

1. *Preparation of Catalysts*

Titanium catalysts which are usually prepared from TiCl$_4$ contain traces of impurities (chlorine and iron ions) and have relatively small surface areas (*2*). To avoid these defects the samples were prepared according to an improved method by coprecipitating nickel and titanium hydroxides* from mixtures of nickel and titanium nitrate solutions with aqueous ammonia at a constant (8.8 ± 0.1) pH. Titanium nitrate solution was prepared beforehand by hydrolyzing pure tetra-*n*-butoxytitanium with

---

* For reasons of brevity the term "titanium hydroxide" will be used to designate hydrated anatase obtained under the present conditions (*3*).

NH_4NO_3 aqueous solution and rapidly dissolving the washed precipitate in a calculated amount of nitric acid. The hydroxides were dried at 50°C and then heated in air at 430°C for 6 hr. Some specimens were fired for 6 hr at 600°C. Table 1 lists the catalysts prepared and the nickel content by chemical analysis.

2. *Procedures*

X-Ray analysis was carried out using an URS-50I (УРС-50И) X-ray unit with Cu $K\alpha$ (Ni-filtered) radiation (*4*).

The thermal analysis was performed on a Paulik, Paulik, Erdey derivatograph.

Surface areas were determined by the BET method with benzene at 20°C for oxides and with air at −196°C for hydroxides (*5*).

A Tesla BS-413 microscope was used to obtain electron micrographs for the samples prepared by a suspension technique (*5*).

Infrared spectra were recorded by an UR-20 (Karl Zeiss, Iena) spectrophotometer. The measurements were made in the range 400–4000 cm^{-1}. Powdered samples were pressed with KBr to prepare transparent discs.

An E6-3 model of teraommeter was used to measure the dc conductivity *in vacuo.* Samples were compressed into tablets under 5×10^3 kg cm^{-2} pressure. Prior to use the contact faces of the tablets were coated with gold evaporated *in vacuo.* The activation energy E_σ of conductivity σ was calculated by the equation

$$\sigma = \sigma_0 e^{E_\sigma/RT} (4,6).$$

The work function of catalysts was determined from the contact potential differences measured by the vibrating condenser technique (*6, 7*).

Magnetic susceptility measurements were carried out using the Faraday method at 400–3800 Oe and 85–540°K (*8*).

ESR spectra were recorded by a РЭ13-01 spectrometer (9.326 MHz) (*8*).

The N_2O decomposition was studied at atmospheric pressure in a flow-circulating system with helium as the carrier gas. The activity is reported as reaction rate related to 1 g of catalyst. Plots of the temperature dependence of reaction rates are used to compare the catalytic properties of samples with different composition (*9*).

II. RESULTS

1. *Phase Relationships*

According to X-ray examinations (Table 1) nickel oxide was the only phase detectable in all 430°C fired samples containing

TABLE 1
X-RAY STRUCTURAL DATA OF $NiO-TiO_2$ CATALYSTS OF 430°C SERIES

Sample No.	NiO content (mol%)	Phase composition		Lattice parameters (Å)[a]			Dispersity (particle mean size) (Å)	
		NiO	TiO_2 (anatase)	NiO	TiO_2 (anatase)		NiO	TiO_2
				a	a	c		
1	0	−	+	—	3.785	9.490	—	150
2	0.97	−	+	—	3.780	9.490	—	140
3	5.4	−	+	—	3.785	9.490	—	140
4	12.1	−	+	—	3.785	9.490	—	100
5	18.0	−	+	—	3.780	9.490	—	125
6	23.5	−	+	—	3.785	9.490	—	75
7	35.3	+	+	4.17	3.78	9.50	80	85
8	60.5	+	−	4.180	—	—	220	—
9	80.5	+	−	4.180	—	—	240	—
10	95.9	+	−	4.175	—	—	250	—
11	100	+	−	4.180	—	—	275	—

[a] Accuracy ± 0.005 Å.

60 mol% or more of NiO. The samples containing less than 35 mol% of NiO showed the presence of anatase as the single distinguishable phase. The existence of both nickel oxide and anatase was observed only in the catalyst with 35 mol% of NiO. It is noteworthy that rutile along with anatase lines were clearly recognized in specimens heated at 600°C and higher. Thus the X-ray analysis of the samples fired at 430°C has not revealed any chemical compounds beside NiO and TiO_2. Also no detectable changes in lattice parameters were found in the samples investigated. Hence, it is conceivable to infer that no solid solutions were formed in the NiO–TiO_2 system. These observations are in accordance with the results described in (*10*, *11*). However the X-ray analysis of the hydroxides indicates readily distinguishable lines at 7.9; 3.96; 2.65 and 1.55 Å which could be ascribed neither to $Ni(OH)_2$ nor to titanium hydroxide and which disappear on heating the samples above 200°C. This observation may suggest the formation of a new hydroxide phase due to the interaction between the hydroxides.

Infrared studies of hydroxides with more than 12 mol% of $Ni(OH)_2$ indicate (Fig. 1a) the existence of the band in the vicinity of 3400 cm^{-1} assignable to the interaction between the hydroxyl groups. The intensity of the band is highest for the samples containing 25–35 mol% of $Ni(OH)_2$. This band, absent in pure hydroxides of nickel and titanium, suggests that the interaction between the components comes into play in the first steps of the catalyst formation. A typical hydroxyl band of $Ni(OH)_2$ at 3040 cm^{-1} was, in addition, noted for the samples with high molar concentration of nickel hydroxide (80%). It would thus appear that two hydroxide phases coexist in the high nickel catalysts.

Infrared spectra of the oxides preheated at 430°C are presented in Fig. 1b. In addition to the usual bands of TiO_2 and NiO, a new weak band at 550–570 cm^{-1} was found for the catalysts with 18 to 80 mol% of NiO assignable to a new compound. This band was much stronger when the samples were preheated at higher temperatures.

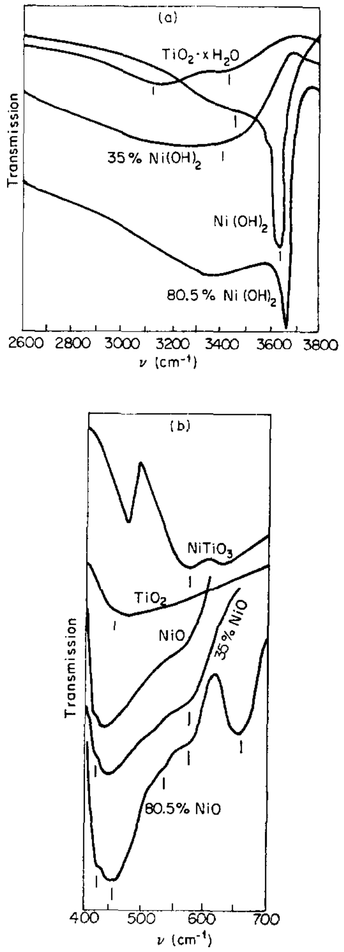

FIG. 1a. Infrared spectra pattern of hydroxides; (b) infrared spectra pattern of oxides.

Differential thermal analysis (DTA) of the hydroxides shows endothermal effects in the region of 100–320°C, apparently caused by dehydration of the samples to the corresponding oxides. Judging by DTA curves, the process associated with water loss in the low nickel samples proceeds in one step, whereas for the 80% $Ni(OH)_2$ sample two steps of dehydration (at 140 and 320°C) can be traced. This situation may arise from the presence of two hydroxide compounds in the high nickel samples.

2. Surface and Texture

The variation of surface area of the oxides and hydroxides as a function of com-

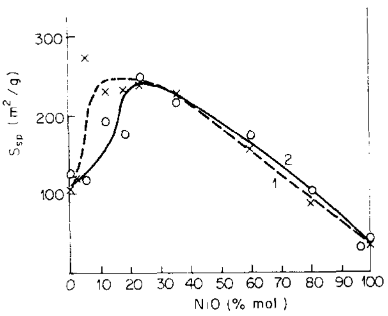

FIG. 2. Change of specific surface areas vs composition: (1) hydroxides; (2) oxides heated at 430°C.

position is presented in Fig. 2. The two curves show a single maximum which lies between 5 and 35% of $Ni(OH)_2$ for hydroxides and between 20 and 35 mol% of NiO for the oxides. Hydroxides and corresponding oxides have nearly the same surface areas except for the 5–18% NiO catalysts, where the oxides possess lower values compared to the hydroxides.

Electron microscopic examination of the hydroxide particles showed them to be of plate and needle shape (Fig. 3a) with the exception of 5–35% $Ni(OH)_2$ samples which show a specific morphology characterized by relatively large porous blocks of 30–50 Å uniform microparticles. This block structure persists in the 23 and 35% NiO samples heated at 430°C (Fig. 3b). The oxides with less than 23% NiO consist of the separate particles of 100–150 Å. The oxide samples containing 60% and more of NiO exhibited two phases: small particles with well-developed surface and large

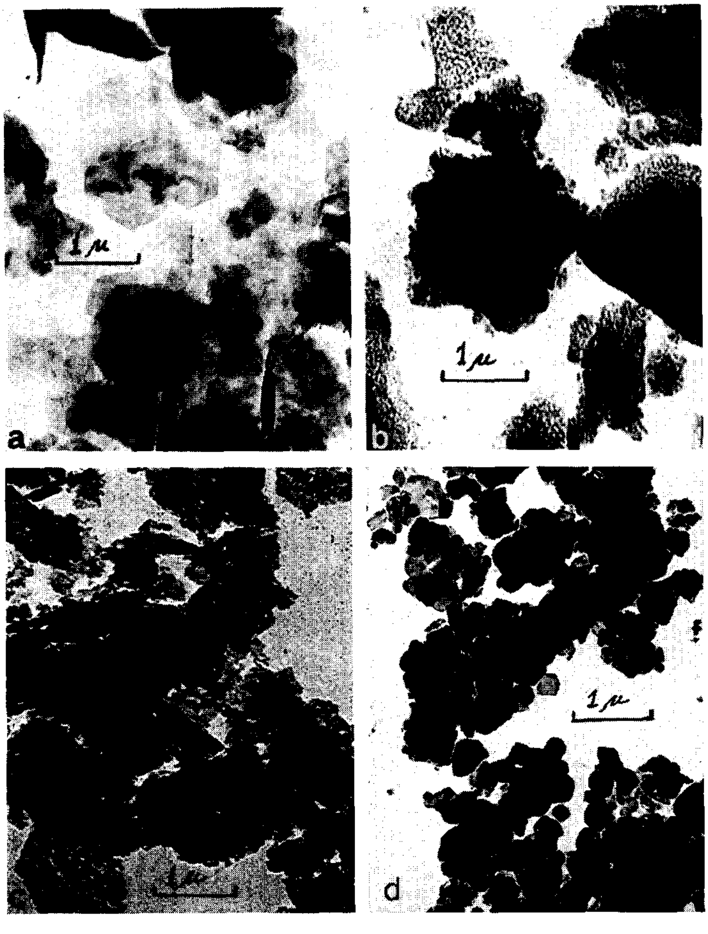

FIG. 3. Electron micrograph patterns: (a) nickel hydroxide; (b) hydroxide sample with 5% $Ni(OH)_2$; (c) catalyst (430°C) with 80.5% NiO; (d) oxide sample with 80.5% NiO calcined at 770°C.

TABLE 2

DISPERSITIES OF SOME NiO–TiO$_2$ CATALYSTS AS DETERMINED BY DIFFERENT METHODS

NiO content (mol%)	Temp of thermal treatment (°C)	Dispersity (particle mean size) (Å)		
		Electron microscopy	X-Ray	Adsorption
0	430	50–150	150	125
5.4	200	30–40	—	70
5.4	430	30–100	140	130
35.3	430	30–50	80	60
80.5	770	200–500	400	—
100	430	100–200	275	220

needles (Fig. 3c). The heat treatment of the samples of 600°C and higher caused growth of crystallites due to sintering (Fig. 3d).

Size distribution data obtained by independent methods (Table 2) show a reasonable agreement, though X-ray analysis and adsorption measurements led to somewhat larger values than electron microscopy.

3. *Electrical and Magnetic Properties*

The variation of the electrical properties of the NiO–TiO$_2$ system as a function of composition proved to be of regular character as is indicated by the curves in Fig. 4. The fall in conductivity, σ, and the corresponding increase of E_σ with the addition of small amounts of either component is consistent with Verwey's (*12*) controlling valency theory. This theory suggests that effects similar to those recorded here are caused by adding small amounts of lower valency ions into the n-semiconductor (Ni^{2+} into TiO_2) and higher valency ions into the p-semiconductor (Ti^{4+} into NiO). However, the interpretation based on electronic effects is justified only if small additions of foreign ions lead to the solid solution formation. Since solid solutions are ruled out by X-ray data, the pattern of conductivity depicted in Fig. 4 requires special consideration which will be given below using the plots of E_σ against the evacuation temperature, T_{vac} for the samples with different composition (Fig. 5).

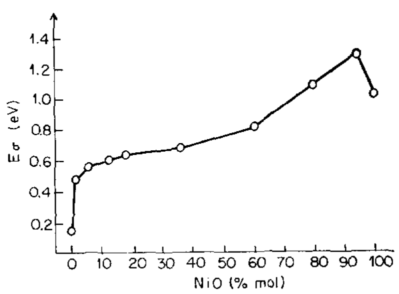

FIG. 4. Conductivity activation energy, E_σ, vs composition of NiO–TiO$_2$ catalysts (heated at 430°C).

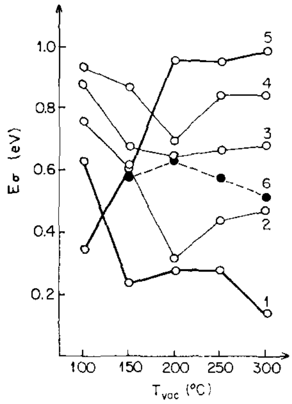

FIG. 5. Different type of E_σ dependence vs *in vacuo* treatment temperature, T_{vac}, for 430°C NiO–TiO$_2$ catalysis: (1) TiO$_2$; (2) 0.97% NiO; (3) 23.5% NiO; (4) 60.5% NiO; (5) NiO; (6) NiO–TiO$_2$ (1:1) mechanical mixture, 430°C.

The work function–composition curve for

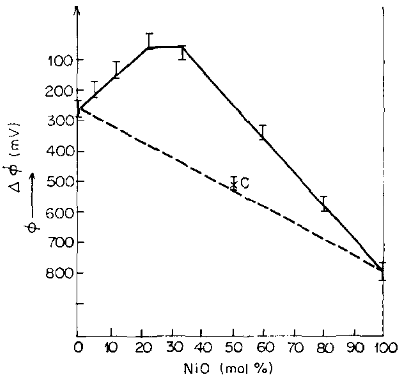

FIG. 6. Changes of work function, $\Delta\phi$, vs composition for NiO–TiO$_2$ catalysis heated at 430°C. Point C—for equimolecular NiO–TiO$_2$ mechanical mixture.

TABLE 3
Magnetic Properties of NiO–TiO$_2$ Catalysts

NiO content (mol%)	Series 430°C: Specific magnetic susceptibility ($\chi_{Ni} \times 10^6$)	Series 430°C: Magnetic moment (μ_B)	Series 430°C: Weiss constant Δ (°K)	Series 800–900°C: Specific magnetic susceptibility ($\chi_{Ni} \times 10^6$)	Series 800–900°C: ESR line width, ΔH (Oe)
5.4	83.5	3.4	0	90.0	700
12.1	57.5	3.1	~0	71.0	700
18.0	74.5	3.2	~0	89.0	700
23.5	76.5	3.3	~0	85.0	770
35.3	77.0	3.3	~0	90.0	650
60.5	28.5	2.0	—[a]	49.5	650
80.5	21.8	1.7	—[a]	25.5	650

[a] The samples do not obey the Curie-Weiss law.

the 430°C preheated oxides shown in Fig. 6 suggests that the work function increases linearly with increasing amounts of nickel and reaches a maximum in the region of 23–35% of NiO. It then decreases linearly with further amounts of nickel. The work function–composition plot obtained shows that the composition of the sample surfaces does not correspond to that indicated by bulk chemical analyses of the samples. If it were the case, the values of the work function would have fallen on the straight line (broken line in Fig. 6). This did occur for a mechanical mixture of NiO and TiO$_2$ (point C) where the correspondence of the chemical composition on the surface and inside the sample is apparent.

The results of magnetic susceptibility measurements for the NiO–TiO$_2$ samples heated at 430°C are reported in Table 3. The values of magnetic moments were found to be about 3.2 μ_B for the oxides with 35% or less of NiO. This indicates octahedral positions of Ni^{2+} ions. The Weiss constant values close to zero imply that Ni^{2+}–Ni^{2+} interactions are unlikely to be substantial in the low nickel catalysts. However, no ESR signal typical of Ni^{2+} ions with a perfect octahedral coordination was observed in the 430°C fired samples, apparently because of the distorted octahedral coordination of Ni^{2+} ions. In fact an ESR signal was readily detectable after the samples have been heated to 600–900°C and diffraction lines due to the perfect NiTiO$_3$ structure could be distinguished by X-ray examination.

As demonstrated by the low values of magnetic susceptibility and magnetic moments a strong interaction between Ni^{2+} ions is developed in the samples containing 60 and 80% NiO. The strong Ni^{2+}–Ni^{2+} interaction is characteristic of fairly large NiO microcrystals.

4. Catalysis

The kinetic results obtained for the N$_2$O decomposition over the NiO–TiO$_2$ samples are shown in Fig. 7. Based on the curves the samples can be classified according to the catalytic activity into two different groups. To the group of the low activity catalysts (curves 1–4) belong the samples containing 0–35% of NiO, whereas the samples with 60% and more of nickel oxide fall into the group of the high activity catalysts (curves 5–7). These results tend to imply that nickel oxide is an active component in the catalysts. However there is no appreciable distinction in catalytic activity between the samples with the NiO content up to 35%† though the X-ray analysis provided a clear indication that the free NiO is present in the low nickel catalysts, particularly, in the sample with

---

† Additional experiments indicated that the technique used in the present study responds to the activity increase induced by the appearance of 1–3% of an active NiO phase in a reference sample.

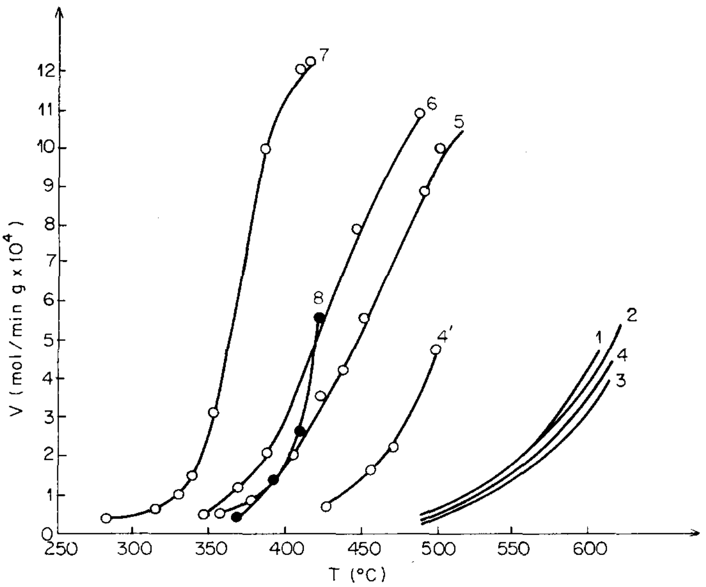

FIG. 7. Activity per unit area of NiO-TiO$_2$ catalysts in N$_2$O decomposition: (1) TiO$_2$; (2) 12.1% NiO; (3) 23.5% NiO; (4) 35.5% NiO; (4′) 35.5% NiO after redox heating treatment; (5) 60.5% NiO; (6) 80.5% NiO; (7) NiO; (8) 35% NiO + 65% TiO$_2$ mechanical mixture.

35% NiO. The system behaves as if the low nickel samples have no substantial concentration of the free nickel oxide on the catalyst surface. The kinetic data obtained for a mechanical mixture (35% NiO and 65% TiO$_2$), which surely contains nickel oxide on the surface, support the different behavior of the coprecipitated (curve 4) and mixed (curve 8) samples with equal nickel concentration. To make nickel oxide in low activity catalysts more accessible for reactants, the coprecipitated sample with 35% of NiO was additionally reduced at 500°C and then oxidized at 280°C. After this treatment the sample was again tested for the N$_2$O decomposition (curve 4′). It can be seen by comparing the curves 4, 4′ and 8 that both the coprecipitated sample subjected to the reducing–oxidizing treatment and the mechanical mixture proved to be much more active than the initial coprecipitated catalyst.

Finally, the observation that the nickel titanate phase was detected in the used catalysts prompted us to estimate catalytic activity of the pure NiTiO$_3$. This was performed with a sample produced by heating an equimolar mixture of NiO and TiO$_2$ at 1250°C. The sample was no more active than pure TiO$_2$.

An additional kinetic investigation described in detail elsewhere (*9*) showed the first order equation $v = kp_{N_2O}$ to be valid for the sample containing 80% of NiO. The activation energy (E_{act}) was calculated to be 53 kcal/mol, not significantly different from the E_{act} [59 kcal/mol (*13*)] obtained for the N$_2$O thermal decomposition, though the rate of thermal decomposition in the present case seems to be negligibly low. This reaction provides therefore an example of the "entropy catalysis," when an increase in the rate of the reaction is caused by the strong increase of the entropy factor of the Arrhenius equation.

III. DISCUSSION

1. Catalyst Formation

From the data described it follows that the addition of TiO$_2$ to NiO as well as NiO to TiO$_2$ results in the enhancement of the oxide surface area (Fig. 1). This observation is similar to those found earlier for other binary oxide systems. Milligan (*14*) postulated that the presence of one oxide may prevent the crystallization of the other and designated this phenomenon as mutual protective action. However, the real mechanism responsible for this phenomenon remains to be understood. Since in the present case the mutual protective action manifests itself already in the hydroxides, the reasons for this phenomenon should be sought at the coprecipitation step. Now we shall consider available data and suggest some possible stages of catalyst formation which seem to clarify the nature of the mutual protection.

Upon coprecipitating from nitrate solutions, the nickel and titanium hydroxides may interact to form hydrous nickel titanate. In confirmation of this suggestion, we can recall infrared data for the hydroxides described in Sect. II,1 and the observation that X-ray diffraction lines of the hydroxides discussed in the same section were similar to those of hydrous nickel aluminate *(15)* and hydrous nickel silicate *(16)*. The formation of hydrous nickel titanate at the coprecipitation step occurs on the surface of the hydroxide particles. Hence hydrous nickel titanate would cover the surface of the hydroxide particles and prevent their further growth and aggregation. As witnessed by the electron micrograph (Fig. 3b) these processes result in the appearance of the porous blocks of microparticles, i.e., a structure with a well-developed surface.

A comparison of specific areas (Fig. 1) indicates that the protective action begins to be operative as soon as 5% $Ni(OH)_2$ was added to titanium hydroxide. However, the well-developed surface appears to be unstable to the action of elevated temperatures in the case of the samples with 5–18% of $Ni(OH)_2$ since on heating at 430°C the resulting surface areas of the oxides were much reduced. With increasing nickel content the particles seem to be more effectively screened by hydrous nickel titanate as indicated by the fact that the samples containing 25 and 35% of $Ni(OH)_2$ showed no observable change in surface areas after heat treatment at 430°C.

As the nickel content exceeds 35% of NiO the surface areas of hydroxides and oxides show the progressive decrease (Fig. 1). To explain this decrease it may be useful to consider results of ir, DTA and electron microscopic examinations. Infrared spectra and thermal analysis show the existence of two different phases in the catalysts with 60% and more of NiO. Electron microscopic examination of these samples (Fig. 3c) indicated needle-shaped particles identified as NiO by X-ray analysis and a phase amorphous to X-rays with a well-developed surface. The latter is held to be nickel titanate formed from the hydrous nickel titanate (see the next section). In the high NiO samples the fraction of the nickel titanate decreases as the nickel content is increased. This is the reason for the decrease in the surface areas.

2. The Main Structural Features

As it follows from the foregoing discussion Verwey's theory of electronic effect of ions with different valency could not be applied to explain the conductivity pattern shown in Fig. 4 because no indication of solid solution was obtained in the $NiO-TiO_2$ system. An agreement between the experimentally observed regularities and the controlling valency rule seems to be of formal character. It is reasonable to seek another possible explanation of observed conductivity pattern based on the compounds which may be formed in the system.

In the current work it was observed that the heat treatment of the samples to temperatures 500°C and higher results in the formation of nickel titanate. At 430°C the samples exhibited only X-ray diffraction patterns corresponding to NiO and/or TiO_2. However we believe that the $NiTiO_3$ phase, which is undetectable by X-rays, can be formed from dehydration of hydrous nickel titanate at temperatures lower than 500°C. Support of this view is given by conductivity measurements and by infrared studies.

If we consider the effect of the vacuum treatment temperature (T_{vac}) on the activation energy of conductivity (E_σ), we can distinguish, by comparing the curves in Fig. 5, three types of patterns. In case of the pure nickel oxide there is a progressive increase in E_σ as T_{vac} was increased. With pure TiO_2 the situation is reversed, whereas for other samples with binary composition the third pattern with a minimum at 200°C is observed. The marked difference between the conductivity patterns obtained for each of the pure oxides, for the mechanical mixture of these oxides (broken line), and for the binary coprecipitated samples makes certain that electrical properties of the samples with binary composition can be attributed to a new compound formed in the system. That this compound is nickel titanate can be concluded from the following argument. The samples preheated at temperatures as high as 600 and 770°C exhibited the conductivity patterns similar to those of the samples heated at 430°C. Because nickel titanate was found by X-ray examination in the samples heated at 500°C and higher, it could conceivably be present in the 430°C fired samples as well. One might therefore think that similar electrical properties of the samples activated at 430°C and at higher temperatures are also associated with the presence of nickel titanate in all binary oxides irrespective of the activation temperature.

It should now be asked why the nickel titanate phase was not detected by X-ray analysis in the samples heated at 430°C. We think that the answer should be found in an irregular defective structure of the $NiTiO_3$ phase which was formed under the present conditions. This view is confirmed by the absence of the ESR signal in the 430°C samples which is expected for the Ni^{2+} ions in the perfectly octahedral coordination (see Sect. II,3). It is only after the sintering at 600°C and higher that the structure becomes more regular and consequently X-ray diffraction lines typical to $NiTiO_3$ and ESR signal are detectable.

The imperfect structure of $NiTiO_3$ undetectable by X-rays in the samples heated at 430°C may be attributed to the fact that nickel titanate was formed as a surface layer on the catalyst particles. This conclusion follows from the change of the conductivity pattern observed on adding as little as 1% of NiO to TiO_2 (Fig. 5, curves 1 and 2). The conductivity pattern of sample with 1% of NiO was found to be similar to that typical for all of the other binary samples ("titanate pattern," curves 2–4). It may be understood if we admit that a small amount of nickel titanate formed in the 1% NiO sample covers the catalyst particles as a surface layer. This picture is so far justified as the electrical conductivity of polycrystalline systems depends principally on the properties of intercrystalline contacts.

Additional information about the distribution of $NiTiO_3$ in the binary samples came from the work function measurements because the presence of the nickel titanate surface layer should affect, in the first place, the surface properties of the specimens. The work function was described (Fig. 6) as increasing linearly with the addition of the first 23% of NiO, then showing a maximum in the region between 23 and 35% of NiO and falling linearly with further amount of NiO. It is known that the work function of the two phase system being plotted against the surface concentration of any phase produces a straight line. We may therefore conclude that there are only two phases (TiO_2 and $NiTiO_3$ rather than NiO) on the surface of catalysts containing up to 23% of NiO and that the fraction of the surface covered by $NiTiO_3$ increases linearly from 0 to 1 as the nickel content increases from 0 to 23% of NiO. Consequently only a fraction of the particle surface is covered by $NiTiO_3$ in the low nickel catalysts. The absence of NiO on the surface of the low nickel catalysts may be supported by comparing the work function patterns for the coprecipitated samples and for the NiO–TiO_2 mechanical mixture (Fig. 6) and by considering catalytic activity data (Sect. II,4).

The samples containing 23–35% of NiO may be considered as consisting of the particles completely covered by nickel titanate. Finally as the nickel content exceeds the 35% NiO level, the free NiO phase together with $NiTiO_3$, appears on the surface of the catalyst. The linear decrease of the work function between 35 and 100% of NiO may be therefore related to the increasing contribution of the free NiO.

The fact that a maximum on the work

function–composition curve is shifted to low nickel concentrations and does not lie at the NiO/TiO_2 equimolar ratio supports an uneven distribution of components on the surface caused by formation of a $NiTiO_3$ surface layer in the low nickel content catalysts.

The free NiO phase which appears on the catalyst surface seems to be responsible for the high catalytic activity of the samples containing more than 35% of NiO but evidently has a minor effect in the conductivity properties. The reason may lie in the isolation of the single NiO patches by the phase with a highly developed surface (Fig. 3c) now attributable to $NiTiO_3$. The lowest conductivity value found for the sample with 94% of NiO can be explained by admitting that the effect of mutual neutralization of current carriers with opposite charges (the holes of NiO and electrons of $NiTiO_3$) was especially pronounced with this specimen.

The presence of nickel titanate in the samples calcined at 430°C is likewise supported by infrared data (Sect. II,1). Binary catalysts of this series exhibited a weak band at 550–570 cm^{-1} (Fig. 1b) which points to the formation of a new compound. This band increases in intensity on heating the samples at temperatures higher than 430°C. Since the same samples yielded X-ray diffraction patterns of $NiTiO_3$ above an activation temperature of 430°C, the band at 550–570 cm^{-1} can be assigned to nickel titanate.

Additional support for this conclusion may be found in the observation that nickel titanate which was pure by X-ray analysis, produced by heating an equimolar mixture of NiO and TiO_2 at 1250°C, showed the same absorption band at 570 cm^{-1} in the infrared spectrum.

3. Role of Structural Features and Electronic Interactions in the Catalysis on $NiO–TiO_2$

The results put forward in this paper provide an essential basis for explanation of the special features in the catalytic behavior of the $NiO–TiO_2$ catalysts. The activity found with the samples containing up to 35% of NiO does not exceed the level of TiO_2 (Fig. 7). We can now explain this peculiarity as due to the fact that nickel occurs only as a low-active nickel titanate on the surface of 1–35% NiO catalysts. The increased activity of the high nickel samples and enhanced activity of the mechanical mixture of NiO and TiO_2 can be attributed to the appearance of the free NiO phase on the catalyst surface. The rise of activity obtained when the 35% NiO coprecipitated sample was subjected to a reducing–oxidizing treatment could be explained by the destruction of the low-active nickel titanate which results in the appearance of a nickel oxide accessible to reactants. Thus NiO is the active phase of $NiO–TiO_2$ system. The other component, titanium oxide, serves apparently to form a specific catalyst structure with the enhanced active surface.

The factors governing the activities of the $NiO–TiO_2$ catalysts in the N_2O decomposition might be also important for the behavior of these solids in other reactions. For example, infrared studies on the activity of $NiO–TiO_2$ catalysts in the isopropyl alcohol decomposition have shown that the presence of the free NiO phase is a necessary prerequisite for the dehydrogenation products to be yielded in detectable amounts.

In seeking to understand the behavior of the NiO catalysts it might be useful to consider how the activity per one surface Ni^{2+} ion changes with progressive dilution of NiO in a matrix of the solid support, i.e., with the decrease of interaction between the Ni^{2+} ions as it was done by Cimino, Schiavello and Stone (*17*) for the NiO–MgO system. However unlike the NiO–MgO catalysts, $NiO–TiO_2$ samples showed no indications of solid solution formation and we therefore are unable to use the approach described in (*17*). Nevertheless, it is not unreasonable to estimate the relative activity of Ni^{2+} ions in nickel titanate. It is obvious, since $NiTiO_3$ is the only phase on the surface of 23 and 35% NiO samples, that catalyst surface units contain Ni^{2+} ions in equal concentration. In view of the fact that the surface areas for both 23 and 35% NiO samples were found to be similar after catalytic experiments (36 and 58 m^2/g), activities per gram of the catalysts can be taken as a measure of the activity per nickel ion. For this reason we are justified in applying the data presented in Fig. 7 to discuss the role played by isolated nickel ions.

A comparison of kinetic data for the samples with 23 and 35% of NiO with corresponding values obtained for pure TiO_2 (curves 1, 3 and 4 in Fig. 7) indicates no appreciable differences in catalytic properties of these specimens. It can be further concluded that weakly interacting Ni^{2+} ions arranged in the network of $NiTiO_3$ are not more active in the N_2O decomposition than Ti^{4+} ions.

This conclusion seems to shed light on the question of whether the catalytic activity of nickel catalysts can be related to local or collective interactions. This problem has been a matter of discussion in recent years (*18*). Some authors (*17*, *19*) studied the catalytic properties of NiO–MgO solid solutions and observed that the activity per nickel ion increased as the interaction between isolated Ni^{2+} ions was reduced by diluting Ni^{2+} ions in the MgO matrix. They arrived at the conclusion that the catalytic activity can be related to local interactions of the isolated Ni^{2+} ions with the reacting molecules. Moreover Cimino, Schiavello *et al.* (*20, 21*) stressed the importance of the geometrical arrangement of Ni^{2+} active sites in the catalysts. They postulated nickel ions in octahedral coordination to be far more important in catalysis than tetrahedrally coordinated nickel ions. In the present case the isolated octahedral Ni^{2+} ions in the network of $NiTiO_3$ provided the basis for the expectation that these ions would especially favor catalytic action. However, low activity of the samples containing nickel titanate indicates the insignificant role of the isolated octahedral Ni^{2+} ions in the N_2O decomposition. Our results tend to imply that collective properties of NiO as the active phase are more essential for catalytic action of the NiO–TiO_2 samples than the local interactions of reactants with the isolated Ni^{2+} ions.

There is of course the possibility that the Ni^{2+} ions, when incorporated in solids of different structure and chemistry, would not react in the same way. Moreover, the notion that $NiTiO_3$ produced by heating NiO and TiO_2 at high temperatures was very active towards carbon monoxide oxidation (*22*) might be understood as evidence in favor of the high selectivity of the catalytic action shown by nickel ions in the same matrix. Considerable caution seems, however, warranted to be positive that the appreciable activity of the catalysts with isolated Ni^{2+} ions can not be ascribed to the action of residual NiO. The presence of free NiO can not be excluded, for instance, in the NiO–ZnO samples because of the insolubility of zinc oxide in nickel oxide (*23*). Besides that, nickel ions might form clusters in the NiO–MgO solid solutions (*24*), whereas nonstoichiometry of the starting mixture of NiO and TiO_2 or the incompleteness of the reaction between them may lead to the occurrence of the excessive NiO phase in the $NiTiO_3$, obtained at the high temperatures.

CONCLUSION

The major results of this study clarified the intimate relations between genetic and structural features and catalytic behavior of the NiO–TiO_2 samples. By coprecipitating the hydroxides, conditions are created favoring the interaction between the constituents of the system. This results in the enhancement of surface areas for the samples with intermediate nickel content due to the phenomenon of mutual protective action which involves the formation of hydrous nickel titanate layer on the surface. The depicted mechanism accounts for the formation of the surface nickel titanate phase at temperatures as low as 430–500°C, whereas the temperatures normally used to prepare $NiTiO_3$ are above 1000°C. We were able to investigate the structural and catalytic properties of "low-temperature" nickel titanate, the structure of which is far from that required by thermodynamic equilibrium.

Kinetic data imply that the catalytic behavior of the system might be related to collective properties of nickel oxide as the active phase rather than to local interactions of reactants with isolated Ni^{2+} ions, arranged in the network of $NiTiO_3$. These Ni^{2+} ions proved to be virtually inactive for the N_2O decomposition.

Our data demonstrate that the poor correlations between catalytic activity and the properties attributable to collective electronic interactions (electrical conductivity, work function) do not generally exclude the importance of collective effects in catalysis.

References

1. Rubinstein, A. M., *Kinet. Catal.* **8**, 1094 (1967).
2. Ganichenko, L. G., Kiselev, V. F., and Murina, V. V., *Kinet. Catal.* **2**, 877 (1961).
3. Danyushevskii, V. Ja., Lafer, L. I., Yakerson, V. I., and Rubinstein, A. M., *Izv. Akad. Nauk SSSR, Ser. Khim.* 1927 (1971).
4. Dulov, A. A., Abramova, L. A., Shashkin, D. P., and Rubinstein, A. M., *Kinet. Catal.* 13, 180 (1972).
5. Dulov, A. A., Dashevskii, M. I., Klyachko-Gurvich, A. L., Slinkin, A. A., and Rubinstein, A. M., *Izv. Akad. Nauk SSSR, Ser. Khim.* 2156 (1972).
6. Dulov, A. A., Abramova, L. A., Gershenzon, I. S., and Rubinstein, A. M., *Dokl. Akad. Nauk SSSR* **210**, 97 (1973).
7. Dulov, A. A., Gershenzon, I. S., and Rubinstein, A. M., *Kinet. Catal.* **15**, 197 (1974).
8. Slinkin, A. A., and Rubinstein, A. M.. *Izv. Akad. Nauk. SSSR, Ser. Khim.* 1831 (1971).
9. Slinkin, A. A., Lavrovskaya, T. K., and Rubinstein, A. M., *Kinet. Catal.* **14,** 1202 (1973).
10. Eremenko, V. N., and Beinish, A. M., *Zh. Neorg. Khim.* **1**, 2119 (1956).
11. Macarovici, C. G., and Zaharescu, M., *Rev. Roum. Chim.* **16**, 577 (1971).
12. Verwey, E. J. W., *Bull. Soc. Chim. Fr.* **D**, 94 (1949).
13. Olschewsky, H. A., Troe, J., and Wagner, H. G., *Ber. Bunsenges. Phys. Chem.* **70**, 450 (1966).
14. Milligan, W. O., *J. Phys. Chem.* **55**, 497 (1951).
15. Akimov, V. M., Slinkin, A. A., Kretalova, L. D., and Rubinstein, A. M., *Izv. Akad. Nauk SSSR, Otd. Khim. Nauk,* 624 (1960).
16. Trombouze, Y., *C. R. Acad. Sci.* **228**, 1432 (1949).
17. Cimino, A., Schiavello, M., and Stone, F. S., *Discuss. Faraday Soc.* **42**, 350 (1966).
18. "Electronic Phenomena in Adsorption and Catalysis on Semiconductors" (Lecture notes, Int. Symp., Moscow, 1968, Ed. T. Volkenshtein) "Mir," Moscow 1969.
19. Keier, N. P., Sazonova, I. S., and Bunina, R. V., *Kinet. Catal.* **10**, 1036 (1969).
20. Schiavello, M., Lo Jacono, M., and Cimino, A., *J. Phys. Chem.* **75**, 1051 (1971).
21. Schiavello, M., Cimino, A., and Criado, J. M., *Gazz. Chim. Ital.* **101**, 47 (1971).
22. Keier, N. P., Sazonova, I. S., Mikhailova. I. L., and Belosludtseva, T. V., *Kinet. Catal.* **7**, 920 (1966).
23. Slinkin, A. A., Rubinstein, A. M., Fedorovskaya, E. A., Shashkin, D. P., Klyachko-Gurvich, A. L., Sagalovich, A. V., and Melnikova, I. V., *Kinet. Catal.* **9**, 88 (1968).
24. Popovskii, V. V., Boreskov, G. K., Muzykantov, V. S., Sazonov, V. A., Panov, G. I., Roschin, V. A., Plyasova, L. M., and Malakhov, V. V., *Kinet. Catal.* **13**, 727 (1972).